Emerging Contaminants 6 (2020) 10–19

Contents lists available at ScienceDirect

Emerging Contaminants

journal homepage: http://www.keaipublishing.com/en/journals/emerging-contaminants/

Research article

Photolysis of hexamethylenediaminetetra(methylenephosphonic acid) (HDTMP) using manganese and hydrogen peroxide

Ramona Kuhn [a, *], Isaac Mbir Bryant [b], Robert Jensch [a], Stephan Liebsch [c], Marion Martienssen [a]

[a] Brandenburg University of Technology Cottbus-Senftenberg, Institute of Environmental Technology and Process Engineering, Chair of Biotechnology of Water Treatment, 03046, Cottbus, Germany
[b] University of Cape Coast, Department of Environmental Science, Cape Coast, Ghana
[c] Zschimmer & Schwarz Mohsdorf GmbH & Co KG, Chemnitztalstr. 1, 09217, Burgstädt, Germany

ARTICLE INFO

Article history:
Received 26 October 2019
Received in revised form
28 November 2019
Accepted 28 November 2019

Keywords:
HDTMP
Hydrogen peroxide
Manganese
LC/MS
Phosphonates
Photolysis

ABSTRACT

Aminophosphonates such as hexamethylenediaminetreta(methylene phosphonic acid) (HDTMP) are categorised as persistent substances. They are commonly used as scale inhibitors in cooling water systems and desalination processes. After utilisation, they are often discharged into aquatic environment without pre-treatment. Advanced oxidation processes (AOP) are promising pre-treatments for industrial wastewater treatments. We investigated the photodegradation of HDTMP with or without addition of manganese ($Mn2^{+}$) and/or H2O2. Similar to results of our former photodegradation studies, we found that HDTMP also undergoes conversion with or without additives during the ultra violet (UV) irradiation. The reaction rate was most affected by the addition of H2O2, i.e. the HDTMP degradation was accelerated by a factor 3.85 compared with UV treatment without additives. The addition of $Mn2^{+}$ accelerated the degradation of HDTMP only by a factor 1.53 compared with the UV treatment without additives. The combined addition of $Mn2^{+}$ and H2O2 accelerated the HDTMP degradation by a factor 2.81.

Interestingly, the initial cleavage is not initiated as expected at the C–N bond but at the C–P bond of the methyl carbon and the phosphorus of the methylenephosphonic acid group of HDTMP. This initial cleavage was independent whether the UV treatment was performed with or without additives. Therefore, we conclude that the degradation mechanism is similar independent of the four tested treatment conditions. We identified amino(methylenephosphonic acid) AMPA, dimethylamino(methylenephosphonic acid) DAMP and iminodi(methylenephosphonic acid) IDMP as the major breakdown products by performing LC/MS analyses. The major mineralisation products were ortho-phosphate, ammonium and carbon dioxide. The mass balances of unknown breakdown products allowed us to speculate about the molecular size of the unknown organic breakdown products.

1. Introduction

The phosphonate hexamethylenediaminetreta (methylene phosphonic acid) (HDTMP) is a common synthetic (poly)amino (poly)phosphonate utilised to prevent scaling of calcium carbonate, calcium sulphate, barium sulphate and ferric oxide [1]. Therefore, HDTMP is commonly applied in oilfield industry, to cooling water systems and desalination processes [2,3]. Like all aminophosphonates, HDTMP is water-soluble, non-volatile and poorly soluble in organic solvents. The direct covalent carbon-to-phosphorus bond provides high chemical stability and high resistance against chemical hydrolysis as well as thermal decomposition [4].

Detailed information on the current consumption of HDTMP are rare to obtain. However, it can be assumed that its consumption increased as well as the consumption and general application of phosphonates in recent decades have been steadily increasing. In fact, their discharge to the environment is critically discussed [5,6]. Rott et al. emphasized that the largest discharge of phosphonates to receiving water is caused by direct discharge of membrane

* Corresponding author.
E-mail address: kuhnr@b-tu.de (R. Kuhn).
Peer review under responsibility of KeAi Communications Co., Ltd.

https://doi.org/10.1016/j.emcon.2019.11.003

Abbreviation

AMPA	amino(methylenephosphonic acid)
ATMP	aminotris(methylenephosphonic acid)
EABMP	ethylamino(bismethylenephosphonic acid)
EDTMP	ethylenediaminetetra(methylenephosphonic acid)
ESI	electrospray ionization
DAMP	dimethylamino(methylenephosphonic acid)
DTPMP	diethylenetriaminepenta(methylenephosphonic acid)
FIDMP	N-formyl iminodi(methylenephosphonic acid)
HMP	hydroxymethylenephosphonic acid
HDTMP	hexamethylenediaminetreta(methylenephosphonic acid)
IDMP	iminodi(methylenephosphonic acid)
LC/MS	liquid chromatography/mass spectrometry
LC-ESI-MS	liquid chromatography-electro spray ionization-mass spectrometry
MADP	methylaminobis(methylenephosphonic acid)
MP	methylphosphonic acid
SIM	selected-ion monitoring

concentrates and cooling water [6]. He averaged discharge loads from 9000 to 18,600 tons per year to rivers in Europe. In the aquatic environment, phosphonates are suspected to serve as long-term contaminations which is why they are categorised as being persistent [7]. For that reason, potential biological degradation of aminophosphonates such as HDTMP was investigated insensitively. In current literature it appears that most scientists focus on deciphering the enzyme regulation of successfully isolated and cultured bacteria. There are only few studies determining the potential and impact of biodegradation in aquatic environments. With regard to HDTMP, there are only few studies reporting only limited or inherent biodegradation [8–10]. Therefore categorising HDTMP as persistent substance is justified or at least as being pseudo-persistent.

As above-mentioned, the enrichment of phosphonates in aquatic environments is mainly caused through the direct discharge of membrane concentrates. Therefore, new approaches such as pre-treatment are intensively investigated [11,12]. Chen et al. [11] investigated the removal of aminotris (methylenephosphonic acid) (ATMP) through chemical adsorption using granular ferric hydroxide. They could show that ATMP absorbed strongly to the granular. However, they concluded that regeneration of the absorbent was inefficient because too many bed volumes (up to 300) were required for generation and they did not also result in complete regeneration. Boels et al. [12] recommended the application of iron-coated filtration sand as low cost absorbent. They emphasized that ATMP was efficiently removable from nanofiltration concentrate when the phosphonate had low concentration, i.e. 12.5 mg L^{-1}. At higher concentration lower maximum adsorption capacity occurred due to competing organic compounds and other effects. Thus, chemical adsorption can be utilised successfully to remove phosphonates from industrial wastewaters at lower concentration.

Alternatively, advanced oxidation processes (AOP) to degrade phosphonates have been investigated. For example, utilisation of ozone (O_3) [13], ultra violet (UV) irradiation [14,15], UV in combination with iron (II) [16,17] and/or UV combined with iron (II) and hydrogen peroxide (H_2O_2) [18,19] were applied. The latter is better known as Photo-Fenton reaction. The application of O_3 was tested with the phosphonate ethylenediaminetetra (methylene phosphonic acid) (EDTMP) which was oxidised within few seconds. The authors predicted the formation of glyphosate and amino (methylenephosphonic acid) (AMPA) which were later confirmed experimentally. Therefore, the use of O_3 might be not favoured. UV degradation of EDTMP and diethylenetriaminepenta (methylenephosphonic acid) (DTPMP) was reported recently [14,15]. The formation of typical breakdown products such as AMPA, iminodi (methylene-phosphonic acid) IDMP and ethylamino (bismethylphosphonic acid) EABMP was reported. The release of the major mineralisation products ortho-phosphate (o-PO_4^{3-}), ammonium (NH_4^+) and carbon dioxide (CO_2) was observed for both EDTMP and DTPMP. In another UV degradation study, the influence of iron under different pH ranges during the photolysis of ATMP, EDTMP, HDTMP and DTPMP was investigated [16]. The authors demonstrated that the addition of iron during the UV treatment enhanced the degradation of the parent compounds. Rott et al. [18] investigated Photo-Fenton reaction in a pure water matrix. He found that under his specific treatment condition ATMP, EDTMP and DTPMP were stable against the UV treatment. He concluded that the applied radiation performance was probably too weak, also the higher pH value (pH 10) prevented complete degradation. Sun et al. [19] also performed UV treatment on common aminophosphonates, but they paid more attention to replacing calcium from the phosphonate complex by ferric iron, which is the higher photo-active complex. They removed UV treated ferric phosphonates by co-precipitation from the wastewater. More than 60% of ATMP was converted to o-PO_4 and overall more than 90% of the total phosphorus was removable from the wastewater effluent.

More recently, Huang et al. reported about the UV/chlorine oxidation of hydroxyethelidene (diphosphonic acid) (HEDP) [20]. They found highest conversion at low chlorine doses and proposed the implementation of this treatment strategy as possible pre-treatment of membrane concentrates controlling the environmental risk by antiscalants. Another combined AOP was introduced by Wang et al. [21], who treated ATMP from desalination concentrates with monochromatic light (254 nm) and addition of persulfate. They proposed to remove those anions prior to the UV/persulfate treatment to improve the complete removal of ATMP.

So far, the application of UV treatment combined with manganese (Mn^{2+}) and/or H_2O_2 to degrade common aminophosphonates such as HDTMP has not been reported. Thus, the aim of this study was to determine the influence of Mn^{2+} and/or H_2O_2 during the photolysis of HDTMP and formation of its major breakdown products and mineralisation products.

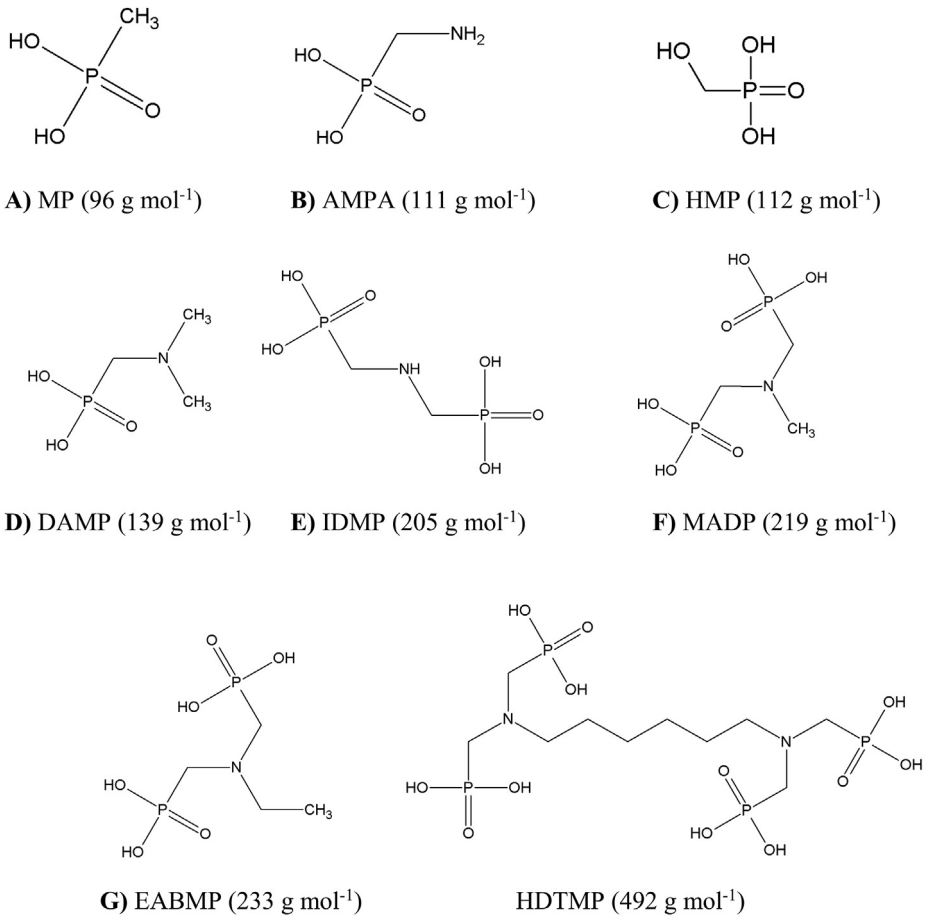

Fig. 1. Standard aminophosphonates used for LC/MS analysis.

2. Material and methods

2.1. Chemicals

HDTMP, EABMP, methylaminobis (methylenephosphonic acid) (MADP), dimethylamino (methylenephosphonic acid) (DAMP), and hydroxymethylenephosphonic acid (HMP) were provided by "Zschimmer & Schwarz Mohsdorf" (Burgstädt, Germany). IDMP, AMPA and methylphosphonic acid (MP) were purchased from Sigma Aldrich (Steinheim, Germany). All structures utilised for this study are shown in Fig. 1. Manganese (II)chloride ($MnCl_2$ x $2H_2O$), hydrogen peroxide (H_2O_2) and potassium bicarbonate ($KHCO_3$) were purchased from Merck (Darmstadt, Germany). Catalase ($\geq$2000 units mg^{-1}) from bovine liver was purchased from Sigma Aldrich (Steinheim, Germany). Ultra-pure water (LC/MS grade) was in-house generated (Adrona Sia Crystal EX, Lithuania). Acetonitrile of LC/MS grade was purchased from VWR (Dresden, Germany), ammonium acetate of analytical grade was purchased from VWR (Leuven, Belgium). All chemicals were of analytical grade or better with purity >99%.

2.2. Experimental setup

The UV degradation experiments without determination of the gas production were all performed in an open quartz glass vessel providing a total liquid volume of 320 mL. The UV degradation experiments with determination of the gas production were all performed in a gas tight vessel providing a total liquid volume of 1000 mL (Fig. 2). All UV experiments were carried out with 100 mg L^{-1} HDTMP (203 μM) dissolved in ultra-pure water. The UV lamp was placed in the centre of the glass (150 W middle pressure mercury lamp; TQ 150 Heraeus Noblelight, Germany). In order to provide a constant room temperature during the entire experiments, the lamp was equipped with a water-cooling jacket. The

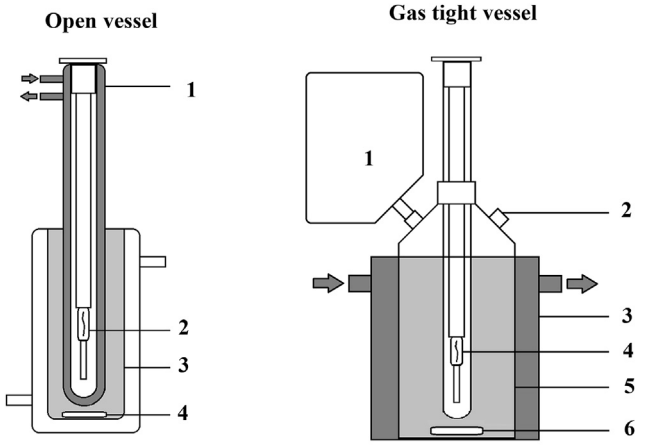

Fig. 2. Scheme of the two system configurations during the UV treatment of 100 mg L^{-1} HDTMP. Legend of system configuration 1 (open vessel) as follows: (1) cooling jacket, (2) UV lamp, (3) vessel, (4) magnetic stirrer. Legend of system configuration 2 (gas tight vessel) as follows: (1) gas bag, (2) gas-tight sampling port, (3) cooling bath, (4) UV lamp, (5) glass bottle, (6) magnetic stirrer.

maximum emission of the lamp was at 366 nm with $4.55 \times 10^{-5} \pm 0.07 \times 10^{-5}$ E s^{-1} incident photon flux, which corresponds to a light intensity of 1.5 mW cm^{-2}. Four different UV treatment conditions were tested including the addition of Mn^{2+}, H_2O_2, Mn^{2+} combined with H_2O_2, and a reference UV treatment without addition of Mn^{2+} and H_2O_2. Manganese was added 1 min before the photolysis experiment was started, i.e. 33 mg L^{-1} $MnCl_2$ x $2H_2O$ (corresponding to 69 μM Mn^{2+}). Hydrogen peroxide was added fresh at the beginning of the UV treatment, i.e. 0.5 mL of 35% peroxide solution was used for the open vessel and 1.56 mL of the gas tight vessel. All UV irradiation experiments were performed in triplicates. The liquid and gas samples were collected at the starting point, after 3 min, 6 min, 10 min, 20 min, 30 min and, then, in 30 min intervals until 300 min. The catalase buffer for the samples of the two UV treatments with H_2O_2 was always prepared fresh before the experiments. The enzyme (0.15 mg mL^{-1}) was dissolved in 0.1 M $KHCO_3$ buffer and 10 μL was added to 1 mL sample to prevent further oxidation. The samples were analysed for HDTMP, EABMP, IDMP, DAMP, HMP, AMPA, and MP, CO_2, methane (CH_4), ethane (C_2H_6), ethylene (C_2H_4), PO_4^{3-}, NH_4^+ and total organic carbon (TOC).

2.3. Analytical methods

HDTMP and its degradation breakdown products were analysed with liquid chromatography-electro spray ionization-mass spectrometry (LC-ESI-MS) using a Finnigan MAT LC/MS (LC spectral system P4000, LCQ MS Detector, autosampler AS 3000, PEEK column SeQuant ZIC-HILIC 150 × 2.1 mm, 3.5 μm/100 Å, Merck, Darmstadt, Germany). Prior to the analyses, all liquid samples were mixed with 50% acetonitrile. The gradient elution was performed in acetonitrile/water at 35 °C at a flow rate of 0.2 mL/min. A mixture of 10% water (solvent A) and 90% acetonitrile (solvent B) was held for 5 min, linearly increased to 60% A within 10 min and held for 5 min, and then further linearly increased to 90% A within 3 min and held for 5 min. The MS detector settings were, as follows: The negative polarity ionization was 3.5 kV and the spray capillary temperature was 220 °C. Selected-ion monitoring (SIM) was selected for quantification. The following mass-to-charge (m/z) ratios were used for identification: HDTMP 492, EABMP 232, MADP 218, IDMP 204, DAMP 138, HMP 111, AMPA 110, and MP 95. For qualitative analyses, full MS scan was used with a mass range between m/z 90 to 650.

The production of CO_2, CH_4, C_2H_6 and C_2H_4 was measured using GC/FID (GC-2014 Shimadzu, Japan; column 3 m 80/100 mesh HayeSep Q 1/8″OD, 2 mm ID, Restek, Bad Homburg, Germany) and GC/ECD for CO_2, respectively. The analysis was performed at 47 °C for 15 min isocratic with helium as the carrier gas. In total, 500 μL gas samples were injected using a Dani headspace-sampler 3950 (Dani, Italy). The headspace temperature was kept at 35 °C.

PO_4^{3-} and NH_4^+ were determined using photometric methods according to the European standard procedures (EN ISO 6878:2004 and DIN 38406 E5, respectively). The samples were measured with a Shimadzu UV-2450 spectrophotometer (Tokyo, Japan). The total organic carbon (TOC) was measured using a TOC analyser DIMATOC 100 (Dimatec Essen, Germany) according to DIN EN 12260.

3. Results

3.1. Determination of quantifiable breakdown products under different UV treatment conditions

We tested the UV degradation of 100 mg L^{-1} HDTMP (corresponding to 24.4 mgC L^{-1}) under four different treatment conditions. Independent whether Mn^{2+} and/or H_2O_2 were added, HDTMP was degradable under all four UV treatment conditions. However, our results of the reference experiment without addition indicate clearly that the phosphonate degraded slowly as compared with the other three treatment conditions (Fig. 3A). In particular, after 210 min UV treatment HDTMP was almost completely degraded. We determined only 0.52 mgC L^{-1} of HDTMP, corresponding to 2.1% of the organic carbon. Assuming a degradation first order, we calculated the degradation rate constant (k_{UV}) to be $6.34 \times 10^{-4} \pm 9.51 \times 10^{-5}$ and the half-life of HDTMP to be 18.5 ± 3.04 min (Table 1). Commonly, chemical reactions in solutions show different reactions order as expected. Chemical reactions following first order are only depending on the concentration of the parent compound. Considering photochemical reaction, i.e. based on radical attack, we could interpret the radial to participate in the degradation reaction as reaction partner. However, the concentration of present radical does not decline because they are constantly release by the UV lamp. Thus, a reaction of pseudo-first order could be assumed. Nevertheless, radicals are not participating the photochemical reaction as real reaction partner and thus we cannot assume pseudo-first order. Therefore we have to assume a first order kinetic.

We also detected some expected breakdown products of HDTMP, but not all. We detected the breakdown products DAMP, IDMP, EABMP and AMPA. In fact, we did not detect the breakdown products MP, HMP and MADP at significant concentrations during all UV treatment conditions. The breakdown product DAMP occurred as the first major breakdown product released within the first 6 min of UV treatment. However, we determined only low concentrations averaging a maximum of 0.31 mgC L^{-1}, corresponding to 1.3% of the organic carbon of the parent compound. Significant release of IDMP and AMPA occurred after 20 min–30 min when the UV treatment was started. The release of IDMP indicated two plateaus, i.e. from 60 to 120 min and then from 150 min to the end of the treatment. The maximum release of IDMP averaged only 1.23 mgC L^{-1} after 300 min UV treatment, corresponding to 5.0%. The maximum release of AMPA was similar to IDMP and averaged 0.92 mgC L^{-1} after 300 min, corresponding to 3.8% of organic carbon respectively.

The UV treatment of HDTMP with addition of Mn^{2+} showed similar trends in the degradation of the parent compound and the release of its major quantifiable breakdown products (Fig. 3B). However, we found that HDTMP was more rapidly degraded. After 90 min of UV treatment, less than 0.66 mgC L^{-1} of HDTMP remained, corresponding to 2.7% of organic carbon respectively. We determined a half-life of 12.10 ± 0.95 min for this treatment condition. We, further, determined IDMP, AMPA and DAMP as major breakdown products while EABMP was almost not quantifiable. We determined the highest release of IDMP after 30 min averaging 0.82 mgC L^{-1}, corresponding to 3.4% of organic carbon respectively. Until 300 min, IDMP was degraded continuously and averaged 0.42 mgC L^{-1}, corresponding to 1.7% respectively. Different to the first UV treatment condition, we found that after 60 min treatment the release of AMPA was always higher compared with the release of IDMP. The highest release AMPA was determined after 120 min averaging 1.38 mgC L^{-1}, corresponding to 5.7% respectively. The breakdown product EABMP was only determinable at trace level.

HDTMP was even more rapidly degraded during the UV treatment with addition of H_2O_2 (Fig. 3C). Under this treatment condition, we determined the fastest degradation kinetic of HDTMP. Reliable quantification of the parent compound was only feasible within the first 15 min of UV treatment determining the half-life which averaged 4.81 ± 0.17 min for HDTMP. Only traces of the parent compound were determinable after 20 min UV treatment averaging 0.12 mgC L^{-1}, corresponding to less than 0.5% respectively. Interestingly, we found the highest release of DAMP and IDMP within the initial 6 min of UV treatment. After 3 min, DAMP

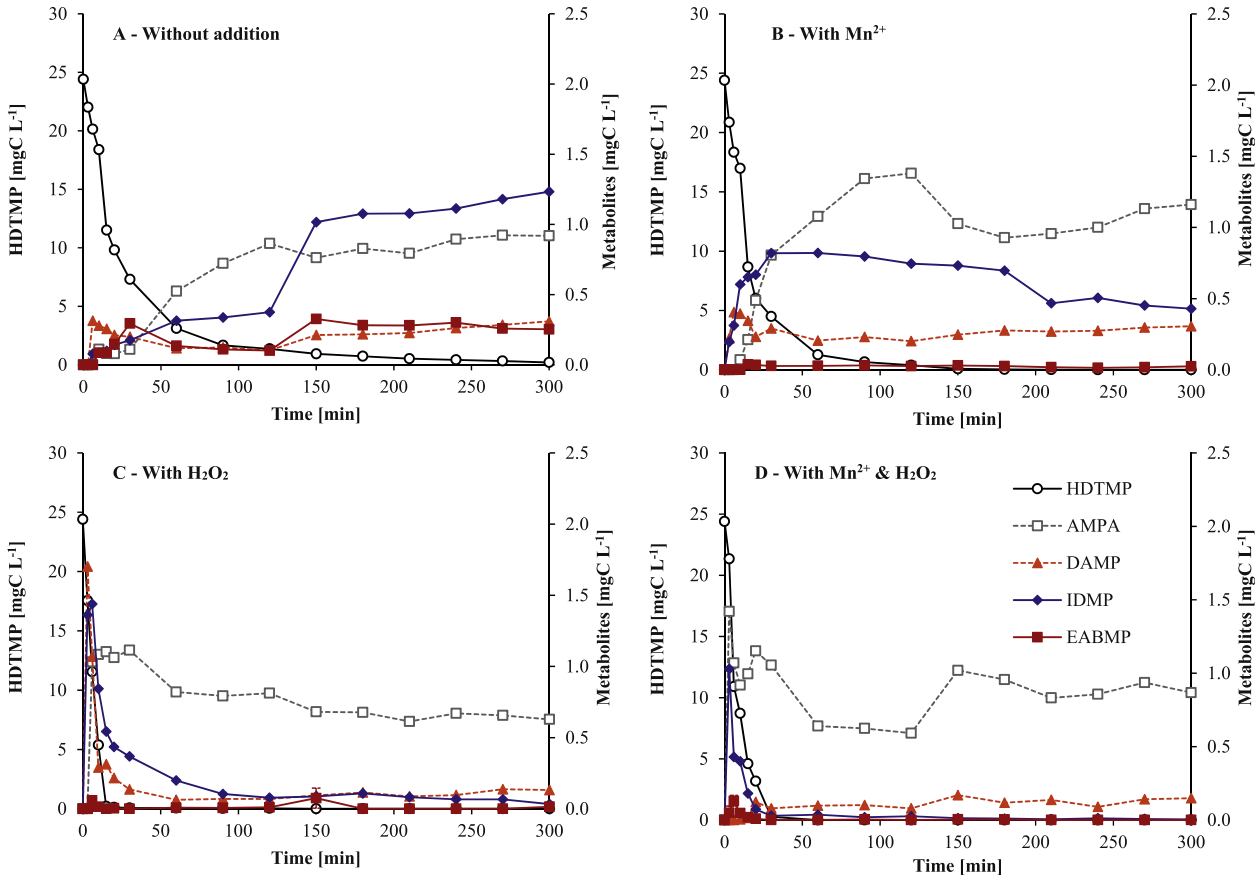

Fig. 3. Photolysis of 100 mg L^{-1} HDTMP without addition (A), with addition of Mn^{2+} (B), with addition of H_2O_2 (C) and with combined addition of Mn^{2+} & H_2O_2 (D).

Table 1
Determined degradation rate constants and half-lives of HDTMP during UV treatment.

	k_{uv} (s^{-1})	Half-life (min)	SSR[a]
Without addition	6.34E-4 ± 9.51E-5	18.52 ± 3.04	386.98 ± 104.21
Mn^{2+}	9.59 E−4 ± 7.23 E−5	12.10 ± 0.95	432.61 ± 248.40
H_2O_2	2.40 E−3 ± 8.39 E−5	4.81 ± 0.17	250.71 ± 133.05
Mn^{2+} & H_2O_2	1.76 E−3 ± 9.17 E−5	6.59 ± 0.34	321.86 ± 33.38

[a] SSR – Sum of squared residuals.

averaged its highest release of 1.70 mgC L^{-1}, corresponding to 7.0% respectively. After 6 min IDMP averaged its highest release of 1.43 mgC L^{-1}, corresponding to 5.9% respectively. We were also capable to determine the half-lives of DAMP and IDMP averaging 1.81 ± 0.20 min and 7.68 ± 0.61 min, respectively. We assumed first order degradation for this calculation. The breakdown product EABMP was not quantified at relevant concentrations and was determined only at traces level. The smallest breakdown product AMPA was determinable during the complete UV treatment and degraded slowly.

The last UV treatment condition, i.e. Mn^{2+} addition combined with H_2O_2, indicated a faster degradation of HDTMP compared with the treatment without addition and also with Mn^{2+}. However, the combination of Mn^{2+} with H_2O_2 did not further promote the degradation kinetic of the parent compound. We determined the half-life of HDTMP averaging 6.59 ± 0.34 min. IDMP and AMPA occurred as the major breakdown products. The latter indicated the highest release of organic carbon after 3 min and averaged 1.42 mgC L^{-1}, corresponding to 5.8%. We were capable to determine the half-life of IDMP for this treatment condition which averaged 4.18 ± 0.34 min. EABMP was only detectable at the beginning of this UV treatment condition and averaged its highest release with 0.13 mgC L^{-1} (corresponding to 0.53%) after 6 min. The half-life of EABMP averaged 2.59 ± 0.28 min. We again assumed for the calculation of the half-lives of both breakdown products again a first order kinetic. We determined constant release of DAMP after 20 min of the treatment until the end.

3.2. Quantification of mineralisation products

We also measured the release of the mineralisation products PO_4–P, NH_4–N and CO_2 (Fig. 4) and proved the statistic significance for selected sample pairs (data not shown). The results confirmed significant differences. As expected, we found the lowest release of PO_4–P for the UV treatment without addition and the fastest for the treatment with the combined addition of Mn^{2+} and H_2O_2 (Fig. 4A). After 300 min treatment, the former treatment condition resulted in 60.9 ± 5.23% PO_4–P released and the latter in 83.6 ± 3.08% PO_4–P released (Table 2). Interestingly, the PO_4–P release of the UV treatment with the combined addition of Mn^{2+} and H_2O_2 indicated the highest release after 3 min, which showed a short decrease until 6 min. We found similar phenomenon of the PO_4–P release for the UV treatment with addition of Mn^{2+}. However, this phenomenon occurred more distinct and with a longer duration during the UV treatment (between 10 min and 30 min). We did not determine such decrease during the UV degradation with addition of H_2O_2. Under this treatment condition, the release of PO_4–P occurred continuously and averaged 81.8 ± 1.29 PO_4–P release after 300 min.

Our results of the NH_4–N release indicated more clearly that

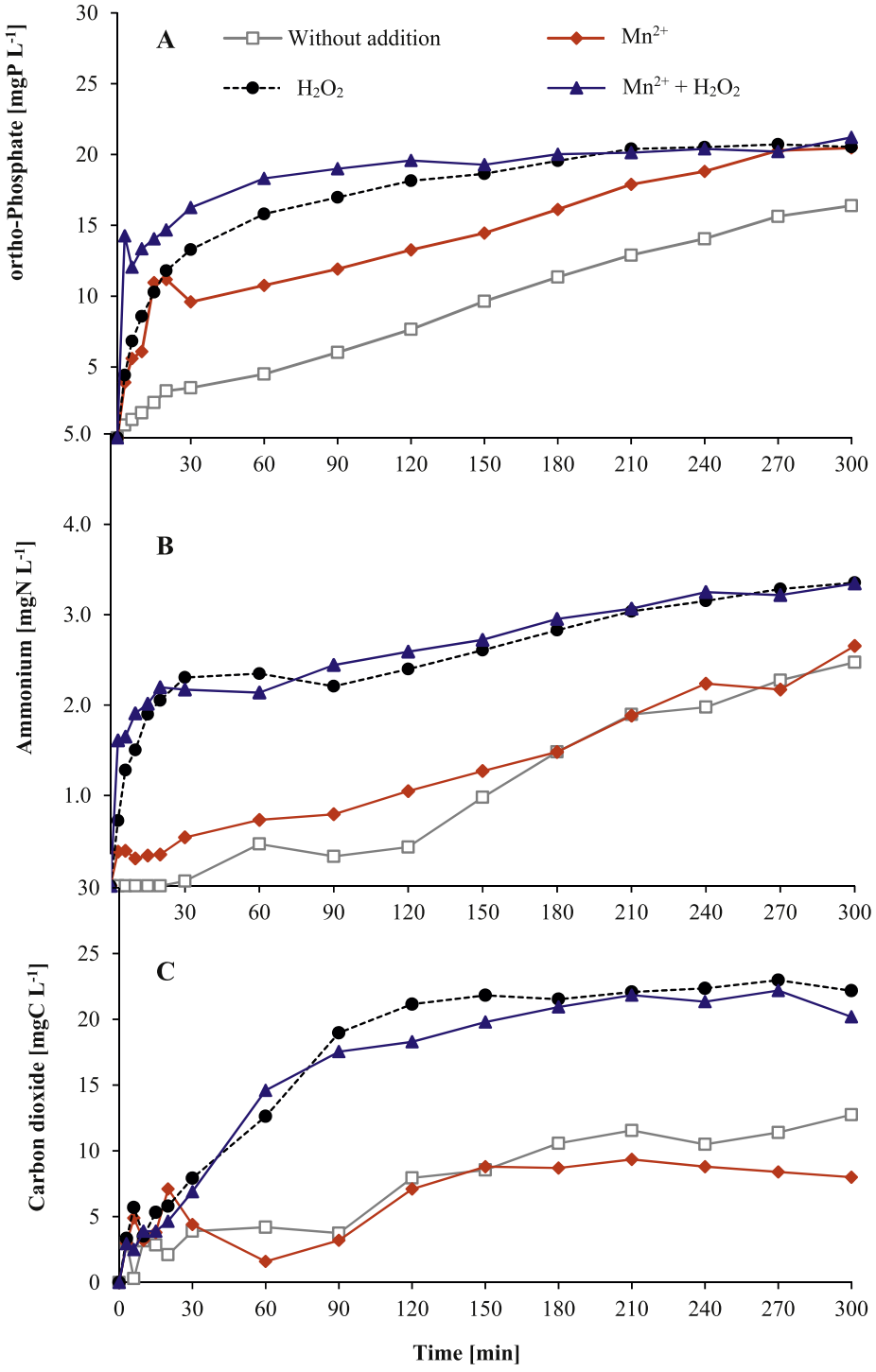

Fig. 4. Release of the mineralisation products PO_4^{3-}, NH_4^+ and CO_2 during the four different UV treatment condition of HDTMP.

Table 2
Release of ortho-phosphate and ammonium, and degradation of organic carbon during UV treatment of HDTMP (100 mg L^{-1}).

	PO_4–P release [%]		NH_4–N release [%]		TOC degradation [%]	
	10 min	300min	10 min	300 min	10 min	300 min
Without addition	6.9 ± 0.66	60.9 ± 5.23	0.0	41.6 ± 2.14	8.7 ± 0.47	47.2 ± 3.57
Mn^{2+}	24.6 ± 1.40	74.5 ± 4.51	4.9 ± 1.43	46.3 ± 2.21	8.9 ± 1.84	24.6 ± 4.00
H_2O_2	33.6 ± 1.34	81.8 ± 1.29	26.4 ± 5.83	54.8 ± 2.68	17.6 ± 3.22	86.6 ± 2.65
Mn^{2+} & H_2O_2	56.3 ± 1.34	83.6 ± 3.08	33.3 ± 3.61	58.3 ± 3.92	15.6 ± 3.18	88.8 ± 2.85

there were obviously two groups with trends of similar degradation pathways (Fig. 4B). In particular, the treatments without addition and with addition of Mn^{2+} showed almost similar NH_4–N releases. After 300 min UV treatment, both treatment conditions averaged 41.6 ± 2.14% and 46.32 ± 2.21% NH_4–N released. The other two UV treatment conditions, i.e. with addition of H_2O_2 and the combination of Mn^{2+} with H_2O_2, indicated both faster and higher releases of NH_4–N. Both treatment conditions averaged at the end of the treatment 54.8 ± 2.68% and 58.3 ± 3.92% NH_4–N released.

In comparison, the release of CO_2 did not indicate such clear trends from the beginning of the UV treatment until 30 min (Fig. 4C). However, when we considered the degradation of the TOC as the source of the CO_2 release (Table 2), we were capable to identify a clearer trend. Thus, the UV treatment without addition showed the lowest degradation of TOC (i.e. 8.7 ± 2.68%) while the UV treatment with H_2O_2 addition showed the highest TOC degradation (i.e. 17.6 ± 3.22%) within the initial 10 min of treatment. Interestingly, after 30 min UV treatment we found again two groups with trends of similar degradation pathways as compared with the release of NH_4–N, i.e. group 1 comprising the UV treatment without addition and with Mn^{2+} and group 2 comprising the UV treatment with addition of H_2O_2 and the combination of Mn^{2+} and H_2O_2. Finally, we determined that almost 90% of the organic carbon was converted to CO_2 for treatment group 2. Against to our expectation, we found the lowest CO_2 release for the treatment condition with Mn^{2+} addition averaging 33% of organic carbon converted to CO_2.

We further evaluated the production of other gases such as CH_4, C_2H_6, and C_2H_4 and found them only at trace level concentrations for the UV treatment without addition. These gases were not detectable in the other UV treatment conditions.

3.3. Mass balance for determination of unknown breakdown products

We, further, evaluated our results based on the data sets of the LC/MS analyses and the measurements of the other parameters (i.e. PO_4–P, NH_4–N, TOC and gas release) in order to balance the development of the sum of the unknown breakdown products during the four different UV treatment conditions. We classified the sum of unknown breakdown products in the three fractions of phosphorus, nitrogen and carbon (Fig. 5A–C).

Our results of the three mass balances indicated that during the UV treatment without addition, the highest quantities of phosphorus containing unknown breakdown products were released, especially from 30 min to 120 min (Fig. 5A). The formation of phosphorus containing unknown breakdown products with the UV treatment with addition of Mn^{2+} indicated indirectly a more rapid degradation of those breakdown products. During the other two treatment conditions, the formation of those breakdown products was significantly lower. Especially the results of the UV treatment with addition of H_2O_2 indicated the formation of phosphorus containing unknown breakdown products at very low concentrations during the complete treatment.

The results of our mass balance of the formation of nitrogen containing unknown breakdown products indicated similar trends for all four UV treatment groups but with different concentrations (Fig. 5B). Thus, all four treatment conditions achieved a maximum release of nitrogen containing unknown breakdown products within the initial 30 min then degraded slowly until the end of the UV treatment.

Surprisingly, the results of our mass balance of the formation of the carbon containing unknown breakdown products indicated clear trends (Fig. 5C). Again, we found two groups with trends of similar degradation pathways. Group 1 comprised again the UV treatment without addition and with Mn^{2+}, and group 2 comprised the UV treatment with addition of H_2O_2 and the combination of Mn^{2+} and H_2O_2.

The formation and degradation of the carbon containing unknown breakdown products occurred notably slower compared with those of group 2. The latter indicated clearly a rapid formation of unknown breakdown products reaching their maximum release at 20 min UV treatment and a rapid degradation achieving almost complete degradation until 300 min.

4. Discussion

Our results evidence that HDTMP undergoes conversion during UV treatment with or without addition of Mn^{2+} and H_2O_2. Therefore, we can assume a similar radical-driven degradation process for UV treated HDTMP (without addition) as we reported recently for EDTMP and DTPMP [14,15]. However in our former studies, we demonstrated that the cleavage of the parent compounds was initiated at the C–N bond yielding high quantities of the breakdown product IDMP and also EABMP. Both IDMP and EABMP are predictable as primary breakdown products of EDTMP and DTPMP due to the chemical structure of both parent compounds. Concerning the chemical structure of HDTMP, the formation of IDMP as breakdown product is also conceivable. The formation of EABMP is rather suspected because the predicted complementary breakdown product of IDMP released from HDTMP ought to be hexylaminobis (methylenephosphonic acid). In this context, the results of our current study confirm the release of IDMP but only small or non-significant yields of EABMP. Nevertheless, we did not identify hexylaminobis (methylenephosphonic acid) as complimentary breakdown product of IDMP.

Furthermore, we found that IDMP was not the initial major breakdown product of HDTMP. Especially for the UV treatment without addition, we identified the breakdown product DAMP being one of the initial breakdown products of HDTMP. During the UV treatment with Mn^{2+} addition and with H_2O_2 addition, we determined high DAMP releases within the initial 10 min. The detection of the breakdown product DAMP implies that the initial cleavage of HDTMP is not taking place at the C–N bond such as demonstrated for EDTMP and DTPMP.

Consequently, we assume that the initial cleavage of HDTMP is subjected to an alternative primary radical attack initiated at the methyl carbon and the phosphorus of the methylenephosphonic acid group, i.e. cleavage at the C–P bond. This breakdown product should have the *m/z* ratio 411. Indeed, we measured high release of *m/z* 411 in all four UV treatments. This breakdown product is then receptive to another radical attack at the central alkyl chain, i.e. between the first and second carbon atoms (C–C bond cleavage), leading to release of DAMP.

In our opinion, this heterolytic cleavage should lead to the release of the complementary breakdown product with the molecular weight of 275 g mol^{-1} (corresponding to *m/z* 274). Unfortunately, we were not capable to detect this breakdown product in the full scan of the MS. Instead, we found several unknown breakdown products only identified as *m/z* ratios (Table S1) indicating strong oxidation such through hydroxylation and carboxylation. Thus, we speculate that the possible breakdown product *m/z* 274 is further degraded. This might be a very rapid oxidation process leading to several still unknown breakdown products.

The formation of oxidised breakdown products during the UV treatment, especially with H_2O_2, might further lead to formation of higher quantities of several organic acids with very low molecular weight such as formic acid and/or acetic acid and others. The formation of such organic acids is not detectable with our LC/MS instrument. However, we recognised rapid decrease of the pH within

the initial 30 min of the UV treatments (Fig. S1). The decrease of the pH for the UV treatment without addition was barely discernible. We, therefore, assume that formation of small organic acids in this treatment condition might be limited through the degradation kinetics of the parent compound preventing rapid acids formation. In fact, our results of the mass balance of the carbon containing unknown breakdown products indicate that the formation of those was lowest for the UV treatment without addition. Low releases of organic carbon can indicate low release of organic acids resulting in almost stable pH during the UV treatment. In comparison, UV treatments of HDTMP with addition of H_2O_2 resulted in rapid release of carbon containing unknown breakdown products within the initial 10 min. The high release of organic carbon can, therefore, indicate high releases of organic acids resulting in rapid pH decrease.

Overall, we found several similar breakdown products only detectable as *m/z* ratio in all four treatment conditions. None of them were quantifiable. We detected most *m/z* ratios for the UV

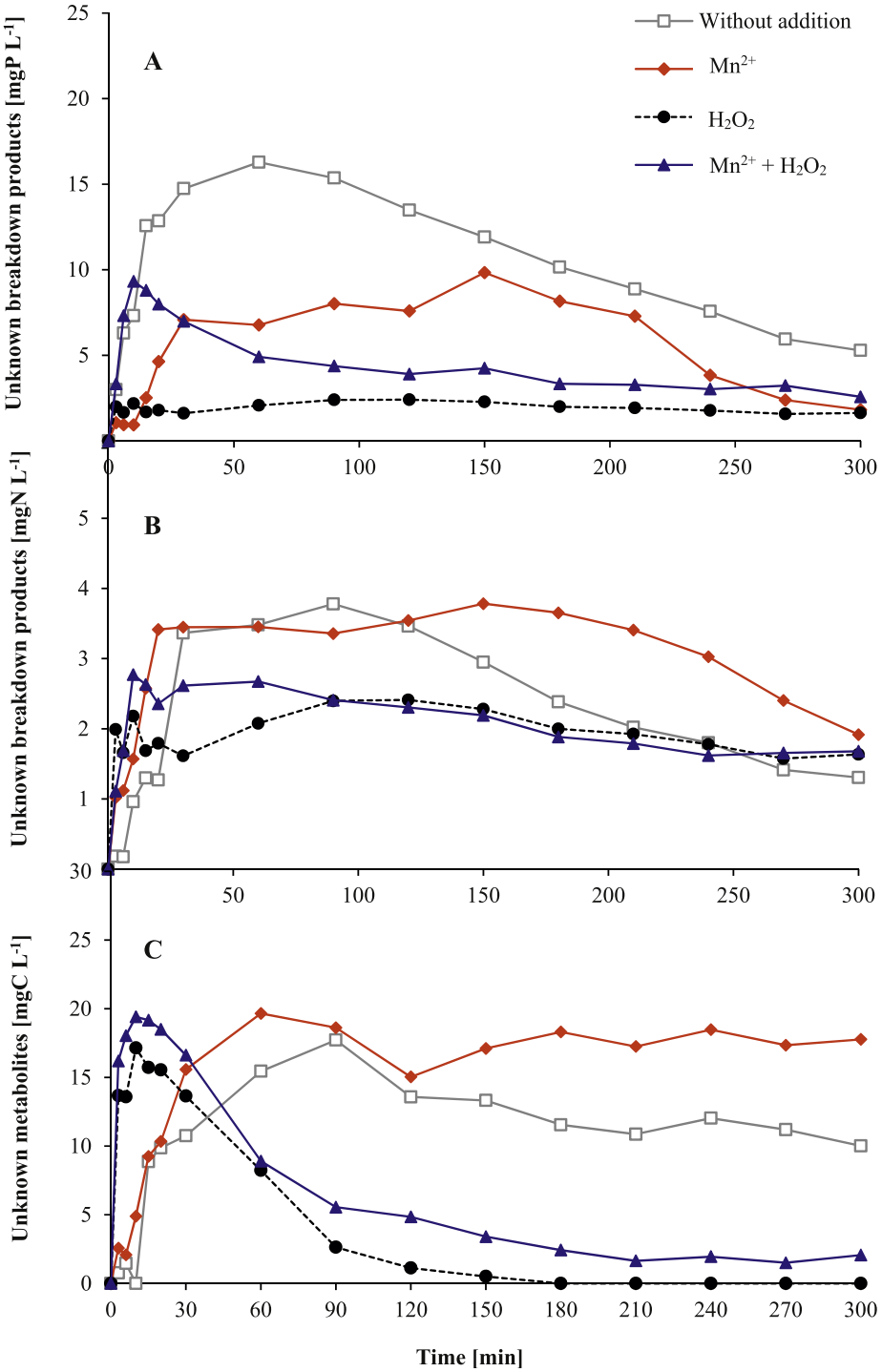

Fig. 5. Mass balance for the sum of phosphorus containing unknown breakdown products (A), sum of nitrogen containing unknown breakdown products (B) and sum of carbon containing unknown breakdown products (C) during UV treatment of HDTMP.

treatment without additives and fewest for the UV treatment with H_2O_2 addition. This finding correlates well with our results of the mass balances of the unknown breakdown products. Possible structures of the detected *m/z* ratios (Table S1) indicate that oxidation through hydroxyl radicals and superoxide radicals as recently reported, seem to play a key role in breaking down the parent compound [22]. We assume that the addition of H_2O_2 resulted in higher yields of hydroxyl radicals promoting the degradation kinetics. Their rapid degradation resulted automatically in fewer detectable breakdown products as compared to the UV treatment without additions.

Thus, we conclude that the degradation mechanism during all four UV treatment conditions was similar and independent of the addition of oxidants and/or catalysts. However, the addition of both Mn^{2+} and/or H_2O_2 has significant influence on the degradation kinetics. For the four treatment conditions, we found in the following order the fastest to the slowest UV degradation of HDTMP: UV with H_2O_2 ≥ UV with H_2O_2 & Mn^{2+} ≥ UV with Mn^{2+} ≥ UV without addition.

4.1. The influence of Mn^{2+} and H_2O_2

We performed our UV treatments with the addition of either Mn^{2+} or H_2O_2. The application of Mn^{2+} to breakdown phosphonates was reported in detail by Nowack and Stone [23–26]. They showed that aminophosphonates were rapidly degraded in the presence of molecular oxygen and Mn^{2+}. In the absence of oxygen no degradation occurred. They concluded that a redox reaction takes place. Thus, Mn^{2+}-catalysed phosphonate degradation requires at least the presence of molecular oxygen. They showed proof that Mn^{2+} reacts as catalyst if the molar ratio is Mn^{2+} ≤ phosphonate [23]. In cases where the molar ratio is Mn^{2+} ≥ phosphonate, they showed that Mn^{2+} can react as strong oxidant [24]. In our study, we conducted our UV treatment experiments with a molar ratio of approximately 0.34 : 1 Mn^{2+}/HDTMP. Therefore, we assume that Mn^{2+} reacts as catalyst in the degradation process. As Nowack and Stone have shown, oxygen is necessary to participate leading to generation of Mn^{2+} for the catalytic reaction [25]. However, the UV treatment can also promote the oxidation of Mn^{2+} to Mn^{3+} [27]. As Nowack and Stone stated, the oxidation of Mn^{2+} is further promoted at relatively low pH and in the presence of phosphonates. During our UV treatments we found similar conditions, i.e. acidic pH, presence of phosphonates and molecular oxygen. Therefore, we conclude that oxidation of Mn^{2+} occurred in the UV treatments. Moreover, we found for only the UV treatment with Mn^{2+} addition decreasing o-PO_4^{3-} concentrations. This spontaneous decrease of free o-PO_4^{3-} was more obvious for the UV treatment with Mn^{2+} addition than for those with the combined addition of Mn^{2+} and H_2O_2. In both cases, it is reasonable to assume that oxidised Mn^{3+} reacted with free o-PO_4^{3-} to form purpurite ($MnPO_4$). Commonly, purpurite precipitates easily. We calculated the maximum yield of potential purpurite formation which resulted in 10 mg L^{-1} in our UV treatment system. Thus, purpurite precipitation in our system could take place without visible evidence. However, the formation of purpurite ought be further evidenced through more detailed investigations. We exclude the formation of birnessite from photooxidised Mn^{2+} as described by Nowack and Stone [23] because cations such as calcium, potassium and sodium required were not available in our treatment conditions.

Furthermore, the reaction of possible purpurite formation occurs more intensively for the UV treatment with only Mn^{2+} addition. This might also explain why the addition of only Mn^{2+} does not further improve the degradation kinetics of HDTMP. In particular, the determined degradation rate constant of UV treated HDTMP with Mn^{2+} addition was increased by factor 1.53 compared with the UV treatment without addition. The UV treatment with H_2O_2 addition was increased by factor 3.85. From these findings, we conclude that the addition of the oxidant H_2O_2 has stronger influence on the degradation kinetics as the addition of the catalyst Mn^{2+}. The combination of both Mn^{2+} and H_2O_2 did not further increase the degradation rate constant. Thus, H_2O_2 was the best additive to rapidly breakdown HDTMP. As state above, H_2O_2 favours the forming of surplus hydroxyl radicals during the UV treatment.

In contrast, it seems that at least the release of the breakdown products AMPA, DAMP and, especially, IDMP are promoted by the presence of Mn^{2+}. We were not capable to further prove the influence on their accelerated degradation through the addition of Mn^{2+}. Nowack and Stone stated that breakdown products such as AMPA and IDMP degrade slower compared to their mother compound in the presence of Mn^{2+} [26]. We had similar observation for UV treated DTPMP with Fe^{2+} addition [15]. However, in our current study the addition of Mn^{2+} might also accelerate both the degradation of the parent compound and the breakdown products. This observation seems to correlate well with the results of the UV treatment with Mn^{2+} addition. For the combined addition, i.e. with Mn^{2+} and H_2O_2, this hypothesis might also be correct since the highest release of AMPA occurred at 3 min of UV treatment indicating accelerated degradation of the parent compound and possible major breakdown products. However, taking into account the results of the mass balances of unknown breakdown products we found the lowest balance gap for the UV treatment with H_2O_2. This indicates that the fastest degradation of HDTMP and all known and unknown breakdown products occurred in fact under this UV treatment condition. Therefore, we can conclude that the degradation might be more accelerated by the addition of H_2O_2 than of Mn^{2+} which confirms indirectly the observation of Nowack and Stone [26]. However, more detailed research on the degradation of quantifiable breakdown products such as AMPA, DAMP and IDMP might be further carried out to determine the influence of Mn^{2+} on the degradation.

Finally, we conclude that UV treated HDTMP with addition of Mn^{2+} improves at least the degradation of the parent compound. We, further, believe that similar influence on the degradation of synthetic aminophosphonates such as HDTMP is presumable in aquatic ecosystems. With regard to technical application, we showed that the degradation through UV irradiation combined with H_2O_2 addition leads to the fastest degradation of HDTMP and its breakdown products. UV treatment combined with Mn^{2+} and H_2O_2 seem not further promote the degradation kinetics of the parent compound. For industrial wastewater pre-treatments, UV irradiation with addition of H_2O_2 as strong oxidant seems to be the best choice of all four tested treatment conditions.

5. Conclusions

The results of our current study show that the aminophosphonate HDTMP is photodegradable with or without addition of Mn^{2+} and/or H_2O_2. The degradation rate of HDTMP is, however, significantly increased by the addition of Mn^{2+} and/or H_2O_2. The degradation of HDTMP was fastest when the UV treatment was combined with H_2O_2 addition. Our results evidence a similar radical-driven degradation mechanism for all four tested UV treatment conditions which leads to release of similar identifiable breakdown products. Different to our former UV treatment studies, we showed proof that the initial cleavage of HDTMP is initiated at the methyl carbon and the phosphorus of the methylenephosphonic acid group, i.e. cleavage at the C–P bond. The decrease of the pH during the initial 30 min for all four treatment conditions indicated the release of organic acids such as formic acid

and/or acetic acid and others.

Finally, we could not identify a similar catalytic effect of Mn^{2+} such as we found for Fe^{2+} during the UV treatment of DTPMP. Furthermore, we found that the addition of Mn^{2+} leads to formation of $MnPO_4$ during UV irradiation, therefore, Mn^{2+} does not participate completely as catalyst. For industrial wastewater pretreatment approaches we propose UV treatment with H_2O_2 addition as strong oxidant.

Funding

This research did not receive any specific grant from funding agencies in the public, commercial, or not-for-profit sectors.

Declaration of competing interest

The authors declare no conflict of interests.

Acknowledgements

The authors thank “Zschimmer & Schwarz” for providing several phosphonate compounds. The authors are grateful to Toni Kestin and Jeansen Emanuel Wen who performed the UV treatment experiments during their master and bachelor project.

Appendix A. Supplementary data

Supplementary data to this article can be found online at https://doi.org/10.1016/j.emcon.2019.11.003.

References

[1] H. Studnik, S. Liebsch, G. Forlani, D. Wieczorek, P. Kafarski, J. Lipok, Amino polyphosphonates – chemical features and practical uses, environmental durability and biodegradation, Nat. Biotechnol. 32 (2015) 1–6, https://doi.org/10.1016/j.nbt.2014.06.007.

[2] P. Zhang, Z. Zhang, Y. Liu, A.T. Kan, M.B. Tomson, Investigation of the impact of ferrous species on the performance of common oilfield scale inhibitors for mineral scale control, J. Pet. Sci. Eng. 172 (2019) 288–296, https://doi.org/10.1016/j.petrol.2018.09.069.

[3] A. Khormali, A.R. Sharifov, D.I. Torba, Increasing efficiency of calcium sulphate prevention using a new mixture of phosphonate scale inhibitors during waterflooding, J. Pet. Sci. Eng. 164 (2018) 245–258, https://doi.org/10.1016/j.petrol.2018.01.055.

[4] A. Obojska, B. Lejczak, M. Kubrak, Degradation of phosphonates by streptomycete isolates, Appl. Microbiol. Biotechnol. 51 (1999) 872–876, https://doi.org/10.1007/s002530051476.

[5] J. Jaworska, H. Van Genderen-Takken, A. Hanstveit, E. van de Plassche, T. Feijtel, Environmental risk assessment of phosphonates, used in domestic laundry and cleaning agents in The Netherlands, Chemosphere 47 (2002) 655–665, https://doi.org/10.1016/S0045-6535(01)00328-9.

[6] E. Rott, H. Steinmetz, J.W. Metzger, Organophosphonates, A review on environmental relevance, biodegradability and removal in wastewater treatment plants, Sci. Total Environ. 615 (2018) 1176–1191, https://doi.org/10.1016/j.scitotenv.2017.09.223.

[7] B. Nowack, Environmental chemistry of phosphonates, Water Res. 37 (2003) 2533–2546, https://doi.org/10.1016/S0043-1354(03)00079-4.

[8] A. Obojska, B. Lejczak, M. Kubrak, Degradation of phosphonates by streptomycete isolates, Appl. Microbiol. Biotechnol. 51 (1999) 872–876, https://doi.org/10.1007/s002530051.

[9] D. Schowanek, W. Verstraete, Phosphonate utilization by bacterial cultures and enrichments from environmental samples, Appl. Environ. Microbiol. 56 (1990) 895–903.

[10] D. Drzyzag, J. Lipok, Analytical insight into degradation processes of aminophosphonates as potential factors that induce cyanobacterial blooms, Environ. Sci. Pollut. Res. 24 (2017) 24364–24375, https://doi.org/10.1017/s11356-017-0068-1.

[11] Y. Chen, J.C. Baygents, J. Farrell, Removing phosphonate antiscalants from membrane concentrate solutions using granular ferric hydroxide, J. Water Proc. Eng. 19 (2017) 18–25, https://doi.org/10.1016/j.jwpe.2017.07.002.

[12] L. Boels, T. Tervahauta, G.J. Witkamp, Adsorptive removal of nitrilotris(methylenephosphonic acid) antiscalant from membrane concentrates by iron-coated waste filtration sand, J. Hazard Mater. 182 (2010) 855–862, https://doi.org/10.1016/j.jhazmat.2010.06.123.

[13] J. Klinger, M. Lang, F. Sacher, H.J. Brauch, D. Maier, E. Worch, Formation of glyphosate and AMPA during ozonation of waters containing ethylenediaminetetra(methylenephosphonic acid), Ozone: Sci. Eng. 20 (1998) 99–110, https://doi.org/10.1080/01919519808547279.

[14] R. Kuhn, E. Tóth, H. Geppert, T. Fischer, M. Martienssen, Identification of the complete photodegradation pathway of ethylenediaminetetra(methylenephosphonic acid) in aquatic solution, Clean Air Soil Water 45 (2017) 1–8, https://doi.org/10.1002/clen.201500774.

[15] R. Kuhn, R. Jensch, I.M. Bryant, T. Fischer, S. Liebsch, M. Martienssen, The influence of selected bivalent metal ions on the photolysis of diethylenetriamine penta(methylenephosphoric acid), Chemosphere 201C (2018) 726–733, https://doi.org/10.1016/j.chemosphere.2018.07.033.

[16] C. Lesueur, M. Pfeffer, M. Fuerhacker, Photodegradation of phosphonates in water, Chemosphere 59 (2005) 685–691, https://doi.org/10.1016/j.chemosphere.2004.10.049.

[17] E. Matthijs, N.T. De Oude, M. Bolte, J. Lemaire, Photodegradation of ferric ethylenediaminetetra(methylenephosphonic acid) (EDTMP) in aquatic solution, Water Res. 23 (1989) 845–851, https://doi.org/10.1016/0043-1354(89)90008-0.

[18] E. Rott, R. Minke, U. Bali, H. Steinmetz, Removal of phosphonates from industrial wastewater with UV/Fe^{II}, Fenton and UV/Fenton treatment, Water Res. 122 (2017) 345–354, https://doi.org/10.1016/j.watres.2017.06.009.

[19] S. Sun, S. Wang, Y. Ye, B. Pan, Highly efficient removal of phosphonates from water by a combined Fe(III)/UV/co-precipitation process, Water Res. 153 (2019) 21–28, https://doi.org/10.1016/j.watres.2019.01.007.

[20] N. Huang, W.L. Wang, Z.B. Xu, Q.Y. Wu, H.Y. Hu, UV/chlorine oxidation of the phosphonate antiscalant 1-hydroxyethane-1,1-diphosphonic acid (HEDP) used for reverse osmosis process: organic phosphorus removal and scale inhibition properties changes, J. Environ. Manag. 237 (2019) 180–186, https://doi.org/10.1016/j.jenvman.2019.02.055.

[21] Z. Wang, G. Chen, G. Patton, C. Ren, H. Liu, Degradation of nitrilotrismethylenephosphonic acid (NTMP) antiscalant via persulfate photolysis: implications on desalination concentrate treatment, Water Res. 159 (2019) 30–37, https://doi.org/10.1016/j.watres.2019.04.051.

[22] R. Kuhn, R. Jensch, I.M. Bryant, T. Fischer, S. Liebsch, M. Martienssen, Photodegradation of ethylenediaminetetra(methylenephosphonic acid) – effect of the system configuration, J. Photochem. Photobiol. A Chem. 388 (2020) 112192, https://doi.org/10.1016/j.jphotochem.2019.112192.

[23] B. Nowack, A.T. Stone, Degradation of nitrilotris(methylenephosphonic acid) and related (amino)phosphonate chelating agents in the presence of manganese and molecular oxygen, Environ. Sci. Technol. 34 (2000) 4759–4765, https://doi.org/10.1021/es0000908.

[24] B. Nowack, A.T. Stone, Homogeneous and heterogeneous oxidation of nitrilotrismethylenephosphonic acid (NTMP) in the presence of manganese(II, III) and molecular oxygen, J. Phys. Chem. B 106 (2002) 6227–6233, https://doi.org/10.1021/jp014293+.

[25] B. Nowack, A.T. Stone, Manganese-catalyzed degradation of phosphonic acids, Environ. Chem. Lett. 1 (2003) 24–31, https://doi.org/10.1007/s10311-002-0014-3.

[26] B. Nowack, A.T. Stone, Oxidative degradation of glyphosate and aminomethylphosphonate by manganese oxide, Environ. Sci. Technol. 39 (2005) 9223–9228, https://doi.org/10.1021/es051342d.

[27] A.D. Anbar, H.D. Holland, The photochemistry of manganese and the origin of the banded iron formation, Geochem. Cosmochim. Acta 56 (1992) 2595–2603, https://doi.org/10.1016/0016-7037(92)90346-K.